
Conditional Lagrangian Wasserstein Flow for Time Series Imputation

Anonymous Author(s)

Affiliation

Address

email

Abstract

1 Time series imputation is important for numerous real-world applications. To
2 overcome the limitations of diffusion model-based imputation methods, e.g., slow
3 convergence in inference, we propose a novel method for time series imputation in
4 this work, called Conditional Lagrangian Wasserstein Flow. The proposed method
5 leverages the (conditional) optimal transport theory to learn the probability flow
6 in a simulation-free manner, in which the initial noise, missing data, and obser-
7 vations are treated as the source distribution, target distribution, and conditional
8 information, respectively. According to the principle of least action in Lagrangian
9 mechanics, we learn the velocity by minimizing the corresponding kinetic energy.
10 Moreover, to incorporate more prior information into the model, we parameterize
11 the derivative of a task-specific potential function via a variational autoencoder,
12 and combine it with the base estimator to formulate a Rao-Blackwellized sampler.
13 The propose model allows us to take less intermediate steps to produce high-quality
14 samples for inference compared to existing diffusion methods. Finally, the experi-
15 mental results on the real-word datasets show that the proposed method achieves
16 competitive performance on time series imputation compared to the state-of-the-art
17 methods.

18 1 Introduction

19 Time series imputation is essential for various practical scenarios in many fields, such as transportation,
20 environment, and medical care, etc. Deep learning-based approaches, such as RNNs, VAEs, and
21 GANs, have been proved to be advantageous compared to traditional machine learning methods on
22 various complex real-words multivariate time series analysis tasks [18]. More recently, diffusion
23 models, such as denoising diffusion probabilistic models (DDPMs) [20] and score-based generative
24 models (SBGMs) [43], have gained more and more attention in the field of time series analysis due to
25 their powerful modelling capability [26, 32].

26 Although many diffusion model-based time series imputation approaches have been proposed and
27 show their advantages compared to conventional deep learning models [44, 11, 12], they are limited
28 to slow convergence or large computational costs. Such limitations may prevent them being applied to
29 real-world applications. To address the aforementioned issues, in this work, we leverage the optimal
30 transport theory [47] and Lagrangian mechanics [3] to propose a novel method, called Conditional
31 Lagrangian Wasserstein Flow (CLWF), for fast and accurate time series imputation.

32 In our method, we treat the multivariate time series imputation task as a conditional optimal transport
33 problem, whereby the random noise is the source distribution, the missing data is the target distribution,
34 and the observed data is the conditional information. To generate new data samples efficiently and
35 accurately, we need to find the shortest path in the probability space according to the optimal transport
36 theory. To this end, we first project the original source and target distributions into the Wasserstein

37 space via sampling mini-batch OT maps. Afterwards, we construct the time-dependent intermediate
 38 samples through interpolating the source distribution and target distribution. Then according to
 39 the principle of least action in Lagrangian mechanics [3], the optimal velocity function moving the
 40 source distribution to the target distribution is learned in a self-supervised manner by minimizing
 41 the corresponding kinetic energy. Moreover, to further improve the model’s performance, we learn
 42 the task-specific potential function by training a Variational Autoencoder (VAE) model [22] on the
 43 observed time series data to build a Rao-Blackwellized trajectory sampler.

44 Finally, CLWF is assessed on two real-word multivariate time series datasets. The obtained results
 45 show that the proposed method achieves competitive performance and admits fast convergence
 46 compared with other state-of-the-art time series imputation methods.

47 The contributions of the paper are summarized as follows:

- 48 • We present Conditional Lagrangian Wasserstein Flow, a novel conditional generative frame-
 49 work based on the optimal transport theory and Lagrangian mechanics;
- 50 • We propose a Rao-Blackwellized trajectory sampler to enhance the data generation perfor-
 51 mance by incorporating the prior information;
- 52 • We develop the practical algorithms to solve the time series imputation problem via a
 53 conditional generative approach;
- 54 • We demonstrate that the proposed method has competitive performance on time series
 55 imputation tasks compared other state-of-the-art methods.

56 2 Preliminaries

57 In this section, we concisely introduce the fundamentals of stochastic differential equations, optimal
 58 transport, Schrödinger Bridge, and Lagrangian mechanics.

59 2.1 Stochastic Differential Equations

60 We treat the data generation task as an initial value problem (IVP), in which $X_0 \in \mathbb{R}^d$ is the initial
 61 data (e.g., some random noise) at the initial time $t = 0$, and $X_T \in \mathbb{R}^d$ is target data at the terminal
 62 time $t = T$. To solve the IVP, we consider a stochastic differential equation (SDE) defined by a Borel
 63 measurable time-dependent drift function $\mu_t : [0, T] \times \mathbb{R}^d \rightarrow \mathbb{R}^d$, and a positive Borel measurable
 64 time-dependent diffusion function $\sigma_t : [0, T] \rightarrow \mathbb{R}_{>0}^d$. Accordingly, the Itô form of the SDE can be
 65 described as follows [36]:

$$dX_t = \mu_t(X_t, t)dt + \sigma_t dW_t, \quad (1)$$

66 where W_t is a Brownian motion/Wiener process. When the diffusion term is not considered, the
 67 SDE degenerates to an ordinary differential equation (ODE). However, we will use the SDE for the
 68 theoretical analysis as it is more general.

69 The Fokker–Planck equation (FPE) [40] describing the evolution of the marginal density $p_t(X_t)$
 70 reads:

$$\frac{\partial}{\partial t} p_t(X_t) = -\nabla \cdot (p_t \mu_t) + \frac{\sigma_t^2}{2} \Delta p_t, \quad (2)$$

71 where $\Delta p_t = \nabla \cdot (\nabla p_t)$ is the Laplacian. In fact, both Eq. eq:sde and Eq. eq:fpe reveal the dynamics
 72 of the system and serve as the boundary conditions for the optimization problems we will introduce in
 73 later sections with different focuses. The differences are when the constraint is Eq. (1), the formalism
 74 is Lagrangian, which depicts the movement of each individual particle; while when the constraint is
 75 Eq.(2), the formalism is Eulerian, which depicts the evolution of population.

76 2.2 Optimal Transport

77 The optimal transport (OT) problem aims to seek the optimal transport plans/ maps that moves the
 78 source distribution to the target distribution [47, 41, 38]. In the Kantorovich’s formulation of the
 79 OT problem, the transport costs are minimized with respect to some probabilistic couplings/joint
 80 distributions [47, 41, 38]. Let p_0 and p_T be two Borel probability measures with finite second

81 moments on the space $\Omega \in \mathbb{R}^d$. $\Pi(p_0, p_T)$ denotes a set of transport plans between these two
 82 marginals. Then, the Kantorovich's OT problem is defined as follows:

$$\inf_{\pi \in \Pi(p_0, p_T)} \int_{\mathcal{X} \times \mathcal{Y}} \frac{1}{2} \|x - y\|^2 \pi(x, y) dx dy, \quad (3)$$

83 where $\Pi(p_0, p_T) = \{\pi \in \mathcal{P}(\mathcal{X} \times \mathcal{Y}) : (\pi^x)_{\#}\pi = p_0, (\pi^y)_{\#}\pi = p_T\}$, with π^x and π^y being two
 84 projections of $\mathcal{X} \times \mathcal{Y}$ on Ω . The minimizer of Eq. (3), π^* , always exist and referred to as the optimal
 85 transport plan.

86 Note that the R.H.S of Eq. (3) can also include an entropy regularization term $D_{\text{KL}}(\pi \| p_0 \otimes p_T)$, then
 87 the original OT problem transforms into the entropy-regularized optimal transport (EROT) problem
 88 with Eq. (2) as the constraint, which frames the transport problem better in terms of convexity and
 89 stability [13] In particular, from a data generation perspective, p_0 is some random initial noise and p_T
 90 is the target data distribution, and we can sample the optimal transport maps in a mini-batch manner
 91 [46, 45, 39].

92 2.3 Schrödinger Bridge

93 The transport problem in Sec. 2.2 can be further viewed from a distribution evolution perspec-
 94 tive, which is particularly suitable for developing the flow models that model the data generation
 95 process. For this reason, the Schrödinger Bridge (SB) problem is introduced [25]. Assume that
 96 $\Omega \in C^1([0, T], \mathbb{R}^d)$, $\mathcal{P}(\Omega)$ is a probability path measure on the path space Ω , then the goal of the SB
 97 problem aims to find the following optimal path measure:

$$\mathbb{P}^* = \arg \min_{\mathbb{P} \in \mathcal{P}(\Omega)} D_{\text{KL}}(\mathbb{P} \| \mathbb{Q}) \quad \text{subject to } \mathbb{P}_0 = q_0 \text{ and } \mathbb{P}_T = q_T, \quad (4)$$

98 where the Kullback–Leibler (KL) divergence $D_{\text{KL}}(\mathbb{P} \| \mathbb{Q}) = \begin{cases} \log \frac{d\mathbb{P}}{d\mathbb{Q}} d\mathbb{P}, & \text{if } \mathbb{P} \ll \mathbb{Q}, \\ +\infty, & \text{otherwise,} \end{cases}$ and \mathbb{Q} is

99 a reference path measure, e.g., Brownian motion or Ornstein-Uhlenbeck process. Moreover, the
 100 distribution matching problem in Eq. (3) can be cast as a dynamical SB problem as well [19, 24, 28]:

$$\arg \min_{\theta} \mathbb{E}_{p(X_t)} \left[\frac{1}{2} \|\mu_t^\theta(X_t, t)\|^2 \right], \quad (5)$$

subject to Eq. (1) or Eq. (2),

101 where θ is the parameters of the variational drift function μ_t .

102 2.4 Lagrangian Mechanics

103 In this section, we formulate the data generation problem under the framework of Lagrangian
 104 mechanics [3]. Let p_t and $\dot{p}_t = \frac{dp_t}{dt}$ be the density and law of the generalized coordinates X_t , respec-
 105 tively. $\mathcal{K}(p_t, \dot{p}_t, t)$ is the kinetic energy, and $\mathcal{U}(p_t, t)$ is the potential energy, then the corresponding
 106 Lagrangian is

$$\mathcal{L}(p_t, \dot{p}_t, t) = \mathcal{K}(p_t, \dot{p}_t, t) - \mathcal{U}(p_t). \quad (6)$$

107 We assume that Eq. (6) is lower semi-continuous (lsc) and strictly convex in \dot{p}_t in the Wasser-
 108 stein space. The kinetic energy $\mathcal{K}(x_t, \mu_t, t)$ and potential energy $\mathcal{U}(p_t, t)$ are defined as follows,
 109 respectively:

$$\mathcal{K}(x_t, \mu_t, t) = \mathbb{E}_{p(X_t)} \left[\int_0^T \int_{\mathbb{R}^d} \frac{1}{2} \|\mu_t(x_t, t)\|^2 dx dt, \right] \quad (7)$$

$$\mathcal{U}(p_t, t) = \mathbb{E}_{p(X_t)} \left[\int_{\mathbb{R}^d} U_t(X_t) \right] dX_t, \quad (8)$$

110 where $U_t(X_t)$ is the potential function. Then the *action* in the context of Lagrangian mechanics is
 111 defined as follow:

$$\mathcal{A}[\mu_t(x)] = \int_0^T \int_{\mathbb{R}^d} \mathcal{L}(x_t, \mu_t, t) dx_t dt. \quad (9)$$

112 According to *the principle of least action*, the shortest path is the one minimizing the action, which is
 113 aligned with Eq. (4) in the SB theory as well. Therefore, we can leverage the Lagrangian dynamics
 114 to tackle the OT problem for data generation. To solve Eq. (6), we need to satisfy the stationary
 115 condition, i.e., the Euler-Lagrangian equation:

$$\frac{d}{dt} \frac{\partial}{\partial \dot{p}_t} \mathcal{L}(x_t, \mu_t, t) = \frac{\partial}{\partial p_t} \mathcal{L}(p_t, \dot{p}_t, t), \quad (10)$$

116 with the boundary condition $\frac{dX_t}{dt} = \mu(X_t, t)$, $q_0 = p_0$, $q_T = p_T$.

117 3 Conditional Lagrangian Wasserstein Flow for Time Series Imputation

118 In the section, building upon the optimal transport theory, the Schrödinger Bridge problem, and
 119 Lagrangian mechanics introduced in Sec. 2, we propose Conditional Lagrangian Wasserstein Flow,
 120 which is a novel conditional generative method for time series imputation.

121 3.1 Time Series Imputation

122 Our goal is to impute the missing time series data points based on the observations. For training,
 123 we adopt a conditionally generative approach for time series imputation in the sample space
 124 $\mathbb{R}^{K \times L}$, where K represents the dimension of the multivariate time series and L represents sequence
 125 length. In our self-supervised learning approach, the total observed data $x^{\text{obs}} \in \mathbb{R}^{K \times L}$ are partitioned
 126 into the imputation target $x^{\text{tar}} \in \mathbb{R}^{K \times L}$ and the conditional data $x^{\text{cond}} \in \mathbb{R}^{K \times L}$.

127 As a result, the missing data points x^{tar} can be generated based on the conditions x^{cond} joint with
 128 some uninformative initial distribution $x_0 \in \mathbb{R}^{K \times L}$ (e.g., Gaussian noise) at time $t = 0$, then the
 129 imputation task can be described as: $x^{\text{tar}} \sim p(x^{\text{tar}} | x_0^{\text{cond}})$, where the total input of the model is
 130 $x_0^{\text{input}} := (x^{\text{cond}}, x_0) \in \mathbb{R}^{K \times L \times 2}$.

131 3.2 Interpolation in Wasserstein Space

132 To solve Eq. (7), we need to sample the intermediate variable X_t in the Wasserstein space first. To do
 133 so, the interpolation method is adopted to construct the intermediate samples. According to the OT
 134 and SB problems introduced in Sec. 2, we define the following time-differentiable interpolant:

$$I_t : \Omega \times \Omega \rightarrow \Omega \quad \text{such that } I_0 = X_0 \text{ and } I_T = X_T, \quad (11)$$

135 where $\Omega \in \mathbb{R}^d$ is the support of the marginals $p_0(X_0)$ and $p_T(X_T)$, as well as the conditional
 136 $p(X_t | X_0, X_T, t)$.

137 For implement I_t , first, we independently sample some random noise $X_0 \sim \mathcal{N}(0, \sigma_0^2)$ at the initial
 138 time $t = 0$ and the data samples $X_T \sim p(x^{\text{tar}})$ at the terminal time $t = T$, respectively. Afterwards,
 139 the interpolation method is used to construct the intermediate samples $X_t \sim p(X_t | X_0, X_T, t)$, where
 140 $t \sim \text{uniform}(0, T)$ [30, 2, 45]. More specifically, we design the following sampling approach:

$$X_t = \frac{t}{T}(X_T + \gamma_t) + (1 - \frac{t}{T})X_0 + \alpha(t) \sqrt{\frac{t(T-t)}{T}} \epsilon, \quad t \in [0, T], \quad (12)$$

141 where $\gamma_t \sim \mathcal{N}(0, \sigma_\gamma^2)$ is some random noise with variance σ_γ injected to the target data samples for
 142 improving the coupling's generalization property, and $\alpha(t) \geq 0$ is a time-dependent scalar.

143 Note that Eq. (12) can only allow us to generate time-dependent intermediate samples in the Euclidean
 144 space but not the Wasserstein space, which can lead to slow convergence as the sampling paths are
 145 not straightened. Hence, to address this issue, we need to project the interpolations in the Wasserstein
 146 space before interpolating to strengthen the probability flow. To this end, we leverage the method
 147 adopted in [46, 45, 39] to sample the optimal mini-batch OT maps between X_0 and X_T first, and
 148 perform the interpolations according to Eq. (12) afterwards. Finally, we have the joint variable
 149 $x_t^{\text{input}} := (x^{\text{cond}}, x_t)$ as the input for computing the velocity of the Wasserstein flow.

150 3.3 Flow Matching

151 To estimate the velocity of the Wasserstein flow $\mu_t(X_t, t)$ in Eq. (1), the previous methods that require
 152 trajectory simulation for training can result in long convergence time and large computational costs

153 [9, 37]. To circumvent the above issues, in this work we adopt a simulation-free training strategy
 154 based on the OT theory introduce in Sec. 2.2 [30, 46, 2], which turns out to be faster and more
 155 scalable to large time series datasets.

156 Since we can now draw mini-batch interpolated samples of the source distribution and target distribu-
 157 tion in the Wasserstein space using Eq. (12), we can model the variational velocity function using a
 158 neural network with parameters θ . Then, according to Eq. (1), the target velocity can be computed
 159 by the difference between the source distribution and target distribution. Therefore, the variational
 160 velocity function $\mu_\theta(x_t^{\text{input}}, t)$ can be learned by

$$\arg \min_{\theta} \int_0^T \int_{\mathbb{R}^d \times \mathbb{R}^d \times \mathbb{R}^d} \left\| \frac{dX_t}{dt} - \mu_\theta^{\theta}(x_t^{\text{input}}, t) \right\|^2 dx_0 dx^{\text{tar}} dx^{\text{input}} dt \quad (13)$$

$$\approx \arg \min_{\theta} \mathbb{E}_{p(x_0), p(x^{\text{tar}}), p(x^{\text{input}}), t} \left[\left\| \frac{x^{\text{tar}} - x_0}{T} - \mu_\theta^{\theta}(x_t^{\text{input}}, t) \right\|^2 \right]. \quad (14)$$

161 Eq. (14) can be solved by drawing mini-batch samples in the Wasserstein space and performing
 162 stochastic gradient descent accordingly. In this fashion, the learning process is simulation-free as the
 163 trajectory simulation is not needed.

164 Moreover, note that that Eq. (13) also obeys the principle of least action introduced in Sec. 2.4 as
 165 it minimizes the kinetic energy described in Eq. (7). Therefore, it indicates that the geodesic that
 166 drives the particles from the source distribution to the target distribution in the OT problem described
 167 in Sec. 2 is found as well, which enables us to generate new samples with less simulation steps
 168 compared to standard diffusion models.

169 3.4 Potential Function

170 So far, we have demonstrated how to leverage the kinetic energy to estimate the velocity in the
 171 Lagrangian described by Eq. 6. Apart from this, we can also incorporate the prior knowledge within
 172 the task-specific potential energy into the dynamics, which enables us to further improve the data
 173 generation performance. To this end, let $U(X_t) : \mathbb{R}^d \times [0, T] \rightarrow \mathbb{R}$ be the task-specific potential
 174 function depending on the generalized coordinates X_t [48, 37, 34]. Therefore, we can compute the
 175 dynamics of the system by

$$\frac{dX_t}{dt} = v_t(X_t, t) = -\nabla_x U_t(X_t). \quad (15)$$

176 Since the data generation problem in our case can also be interpreted as a stochastic optimal control
 177 (SOC) problem [4, 17, 35, 50, 21, 5], then the existence of such $U_t(X_t)$ is assured by Pontryagin’s
 178 Maximum Principle (PMP) [16].

179 To estimate $v_t(X_t, t)$, according to the Lagrangian Eq. (6), we assume that the potential function
 180 takes the form $U_t(X_t) \approx -\log \mathcal{N}(X_t | \hat{X}_t, \sigma_p^2)$, where \hat{X}_t the learned mean and σ_p^2 is the pre-defined
 181 variance. As a result, the derivative is $\nabla_x U(X_t) = \frac{X_t - \hat{X}_t}{\sigma_p^2}$. In terms of practical implementation, we
 182 parameterize $\nabla_x U(X_t)$ via a Variational Autoencoder (VAE) [22]. More specifically, we pre-train a
 183 VAE on the total observed time series data X^{obs} . Afterwards, the reconstruction discrepancies of the
 184 VAE are used to approximate the task-specific $v^\phi(X_t, t)$ depending on X_t :

$$v_t^\phi(X_t, t) = -\frac{1}{\sigma_p^2}(X_t - \text{VAE}(X_t)), \quad (16)$$

185 where $\text{VAE}(X_t)$ represents the reconstruction output of the pre-trained VAE model with input X_t ,
 186 and σ_p^2 is treated as a positive constant for simplicity. In this manner, we can incorporate the prior
 187 knowledge learned from the accessible training data into the sampling process formulated by Eq. (14)
 188 to enhance the data generation performance.

189 3.5 Rao-Blackwellized Sampler

190 To generate the missing time series datapoints, we first formulate an unbiased ODE sampler
 191 $S(X_t, \mu_t^\theta(X_t, t), t)$ for X_{t+1} with the Euler method and $\mu_t^\theta(X_t, t)$ learned by Eq. (14) (which

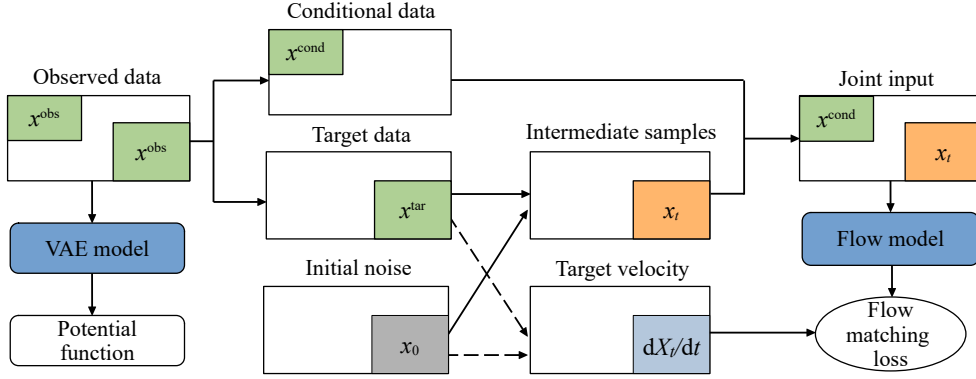


Figure 1: The overall training process of Conditional Lagrangian Wasserstein Flow.

192 means the diffusion term in Eq. 1 is omitted). Alternatively, one can also adopt the SDE sampler by
 193 using the Euler–Maruyama method. Nevertheless, to ensure achieve the best imputation performance,
 194 we choose the ODE sampler for implementation. Note that the ODE sampler alone is good enough to
 195 generate high-quality samples for time series imputation.

196 Now we can construct a Rao-Blackwellized trajectory sampler [8] for time series data imputation
 197 using Eq. 14 and Eq. 16. To this end, we first treat $\mathcal{S}(X_{t+1}|X_t, \mu_t^\theta(X_t, t), t)$ be the base estimator
 198 for X_{t+1} with $\mathbb{E}[\mathcal{S}^2] < \infty$ for all X_{t+1} . And we assume $\mathcal{T}(X_t, v_t^\phi(x_t, t), t)$ is a sufficient statistic
 199 for X_{t+1} based on Eq. 16, even it is not a very accurate estimator for X_{t+1} . As a result, we can
 200 formulate a new trajectory sampler $\mathcal{S}^* = \mathbb{E}[\mathcal{S}|\mathcal{T}]$ to generate the missing time series data. Then
 201 according to the Rao-Blackwell theorem [8], we have

$$\mathbb{E}[\mathcal{S}^* - X_{t+1}]^2 \leq \mathbb{E}[\mathcal{S} - X_{t+1}]^2, \quad (17)$$

202 where the inequality is strict unless \mathcal{S} is a function of \mathcal{T} . Eq. 17 suggests we can construct a more
 203 powerful sampler with smaller errors than the base ODE sampler \mathcal{S} using Rao-Blackwellization.

204 3.6 The Algorithms

205 The overall training process of CLWF is illustrated in Fig. 1, which consists of the following
 206 stages. First, the total observed data x^{obs} are partitioned into the target data and conditional data for
 207 training. Next, the data pairs of x^{tar} and x_0 are sampled from the target dataset and random Gaussian
 208 noise, respectively. Then, the data pairs are projected into the Wasserstein space by sampling the
 209 corresponding OT maps. After that, the intermediate variable x_t is sampled through interpolation
 210 using Eq. (12). We can approximate the target velocity $\frac{dX_t}{dt}$ by computing $\frac{x^{\text{tar}} - x_0}{T}$. Subsequently,
 211 we use the joint distribution of the conditional information x^{cond} and the intermediate variable x_t ,
 212 x^{input} as the total input to feed the variational flow model μ_t^θ to compute the velocity. And the flow
 213 matching loss defined by Eq. (14) is minimized by stochastic gradient descent.

214 Furthermore, to incorporate the prior information of into the model, we can choose to train a VAE
 215 model on the total observed data x^{obs} . This is used to estimate the derivative of the task-specific
 216 potential function according to Eq. (16), which can be further utilized to construct a more powerful
 217 Rao-Blackwellized sampler for inference.

218 For inference, at time $t = 0$, we sample the initial random noise x_0 and conditional information
 219 x^{cond} to formulate the joint variable x^{input} . Note that during the trajectory sampling x_0 will evolve
 220 over time, while x^{cond} remain invariant. We use x^{input} as the input of the flow model μ_t^θ to compute
 221 the velocity. Afterwards, we sample the new x_t using the Euler method. If we perform Rao-
 222 Blackwellization, then x_t is fed to the VAE model for computing the derivative of the potential
 223 function, and x_t is updated again using the Euler method. The above process will be repeated until
 224 reach its convergence. Moreover, we can sample multiple trajectories using different initial random

225 noise, and the averages as the final imputation results. Finally, the proposed training and sampling
 226 procedures are presented in Algorithm 1 and Algorithm 2, respectively.

Algorithm 1 Training procedure

Require: Terminal time: T , max epochs, observed data X^{obs} , parameters: θ and ϕ .
while epoch < max epochs **do**
 227 sample t , (x_0, x_T) , and OT maps;
 sample x_t according to Eq. (12);
 minimize Eq. (14);
end while
if Rao-Blackwellization **then**
 train a VAE model on X^{obs} .
end if

Algorithm 2 Sampling procedure

Require: initial time $t = 0$, terminal time: $T = 1$, Euler method step number: N .
 sample initial noise $X_0 \sim \mathcal{N}(0, \sigma_0^2)$
while $t < T$ **do**
 $X_t = X_t + \mu_t^\theta(x^{\text{input}}, t) \frac{T}{N}$
 if Rao-Blackwellization **then**
 $X_t = X_t + v_t^\phi(x_t, t) \frac{T}{N}$
 end if
 $t = t + \frac{T}{N}$
end while

228 4 Experiments

229 4.1 Datasets

230 We use two public multivariate time series datasets for validation. The first dataset is the PM 2.5
 231 dataset [51] from the air quality monitoring sites for 12 months. The missing rate of the raw data
 232 is 13%. The feature number K is 36 and the sequence length L is 36. In our experiments, only the
 233 observed datapoints are masked randomly as the imputation targets.

234 The other dataset we use is the PhysioNet dataset [42] collected from the intensive care unit for 48
 235 hours. The feature number K is 35 and the sequence length L is 48. The missing rate of the raw data
 236 is 80%. In our experiments, 10% and 50% of the datapoints are masked randomly as the imputation
 237 targets, which are denoted as PhysioNet 0.1 and PhysioNet 0.5, respectively.

238 4.2 Baselines

239 For comparison, we select the following state-of-the-art timer series imputation methods as the
 240 baselines: 1) GP-VAE [18], which is combines a VAE model and a Gaussian Process prior; 2)
 241 CSDI [44], which is based on the conditional diffusion model; 3) CSBI [12], which is based on the
 242 Schrödinger bridge diffusion model; 4) DSPD-GP [7], which combines the diffusion model with the
 243 Gaussian Process prior.

244 4.3 Experimental Settings

245 In terms of the choices of architectures, both the flow model and the VAE model are built upon
 246 Transformers [44]. We use the ODE sampler for inference and sample the exact optimal transport
 247 maps for interpolations to achieve the optimal performance. The optimizer is Adam and the learning
 248 rate: 0.001 with linear scheduler. The maximum training epochs is 200. The mini batch size for
 249 training is 64. The total step number of the Euler method used in CLWF is 15, while the total step
 250 numbers for other diffusion models. i.e., is CSDI, CSBI, and DSPD-GP are 15 (as suggested in their
 251 papers). The number of the Monte Carlo samples for inference is 50. The standard deviation σ_0
 252 for the initial noise X_0 is 0.1, and the standard deviation σ_γ for the injected noise γ_t 0.001. The
 253 coefficient σ_p^2 in the derivative of the potential function is 0.01.

254 4.4 Experimental Results

255 4.4.1 Imputation Results

256 We assess the proposed method on PM 2.5, PhysioNet 0.1 and PhysioNet 0.5, respectively. The root
 257 means squared error (RMSE) and mean absolute error (MAE) are used as the evaluation metrics.
 258 From the test results shown in Table 1 and Fig. 2, we can see that our method CLWF outperforms
 259 the existing deep learning-based method (GP-VAE) and the recent state-of-the-art diffusion methods
 260 (CSDI, CSBI, and DSPD-GP). Moreover, CLWF uses only 15 sampling steps for inference, while the

Table 1: Test imputation results on PM 2.5, PhysioNet 0.1, and PhysioNet 0.5 (5-trial averages). The best are in bold and the second best are underlined.

Method	PM 2.5		PhysioNet 0.1		PhysioNet 0.5	
	RMSE	MAE	RMSE	MAE	RMSE	MAE
GP-VAE	43.1	26.4	0.73	0.42	0.76	0.47
CSDI	19.3	9.86	0.57	0.24	0.65	0.32
CSBI	19.0	<u>9.80</u>	0.55	<u>0.23</u>	0.63	0.31
DSPD-GP	<u>18.3</u>	9.70	<u>0.54</u>	0.22	0.68	<u>0.30</u>
CLWF	18.1	9.70	0.47	0.22	<u>0.64</u>	0.29

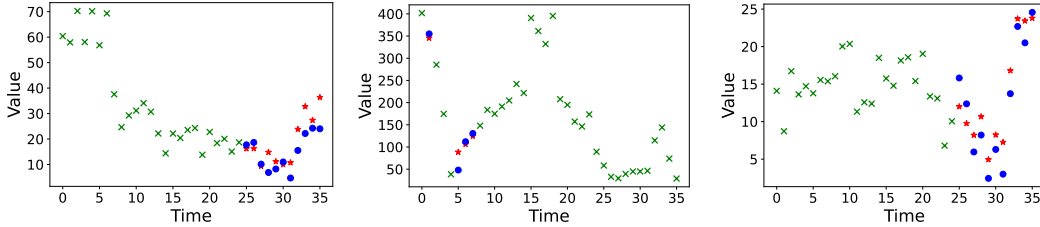


Figure 2: Visualization of the test imputation results on PM 2.5, green dots are the conditions, blue dots are the imputation results, and red dots are the ground truth.

Table 2: Single-sample test imputation results on PM 2.5, PhysioNet 0.1, and PhysioNet 0.5 (5-trial averages).

Method	PM 2.5		PhysioNet 0.1		PhysioNet 0.5	
	RMSE	MAE	RMSE	MAE	RMSE	MAE
CSDI	22.2	11.7	0.74	0.30	0.83	0.40
CLWF	18.4	10.0	0.48	0.22	0.64	0.30

261 baseline diffusion method uses only 50 sampling steps. This suggests that CLWF is faster and more
 262 accurate than the existing methods on time series imputation tasks.

263 4.4.2 Ablation Study

264 **Single-sample Imputation Result.** We compare the time series imputation performance of CLWF
 265 with CSDI using only one Monte Carlo sample. The test results shown in Table 2 shows that CWFL
 266 outperforms CSDI, which suggests that CWFL exhibits lower imputation variances compared to
 267 diffusion-based models. This indicates that CWFL is more efficient and computationally economical
 268 for inference.

Effect of Rao-Blackwellization. We compare the test imputation CLWF with and without using Rao-Blackwellization. Note that the PhysioNet dataset does not have enough non-zero data points to train a valid VAE model, therefore we only construct the Rao-Blackwellized sampler for the PM 2.5 dataset. The results showed in Table 3 indicates that the Rao-Blackwellized sampler can further improve the time series imputation performance of the base sampler.

Table 3: Test imputation results on PM 2.5 (5-trial averages).

Method	PM 2.5	
	RMSE	MAE
CLWF (without RB)	18.2	9.75
CLWF (RB)	18.1	9.70

269 **5 Related Work**

270 **5.1 Diffusion Models**

271 Diffusion models, such as DDPMs [20] and SBGM [43], are considered as the new contenders
272 to GANs on data generation tasks. But they generally take relatively long time to produce high
273 quality samples. To mitigate this problem, the flowing matching methods have been proposed from
274 an optimal transport. For example, ENOT uses the saddle point reformulation of the OT problem to
275 develop a new diffusion model [19] The flowing matching methods have also been proposed based
276 on the OT theory [27, 29, 31, 2, 1]. In particular, mini-batch couplings are proposed to straighten the
277 probability flows for fast inference [39, 45, 46].

278 The Schrödinger Bridge have also been applied to diffusion models for improving the data generation
279 performance of diffusion models. Diffusion Schrödinger Bridge utilizes the Iterative Proportional
280 Fitting (IPF) method to solve the SB problem [14]. SB-FBSDE proposes to use forward-backward
281 (FB) SDE theory to solve the SB problem through likelihood training [10]. GSBM formulates a
282 generalized Schrödinger Bridge matching framework by including the task-specific state costs for
283 various data generation tasks [28] NLSB chooses to model the potential function rather than the
284 velocity function to solve the Lagrangian SB problem [24]. Action Matching [33, 34] leverages
285 the principle of least action in Lagrangian mechanics to implicitly model the velocity function for
286 trajectory inference. Another classes of diffusion models have also been proposed from an stochastic
287 optimal control perspective by solving the HJB-PDEs [35, 50, 5, 28].

288 **5.2 Time Series Imputation**

289 Many diffusion-based models have been recently proposed for time series imputation [26, 32]. For
290 instance, CSDI [44] combines a conditional DDPM with a Transformer model to impute time series
291 data. CSBI [12] adopts the FB-SDE theory to train the conditional Schrödinger bridge model to for
292 probabilistic time series imputation. To model the dynamics of time series from irregular sampled
293 data, DSPD-GP [7] uses a Gaussian process as the noise generator. TDdiff [23] utilizes self guidance
294 and learned implicit probability density to improve the time series imputation performance of the
295 diffusion models. However, the time series imputation methods mentioned above exhibit common
296 issues, such as slow convergence, similar to many diffusion models. Therefore, in this work, we
297 proposed CLWF to tackle these challenges.

298 **6 Conclusion, Limitation, and Broader Impact**

299 In this work, we proposed CLWF, a novel time series imputation method based on the optimal
300 transport theory and Lagrangian mechanics. To generate the missing time series data, following the
301 principle of least action, CLWF learns a velocity field by minimizing the kinetic energy to move
302 the initial random noise to the target distribution. Moreover, we can also estimate the derivative of
303 a potential function via a VAE model trained on the observed training data to further improve the
304 performance of the base sampler by Rao-Blackwellization. In contrast with previous diffusion-based
305 models, the proposed requires less simulation steps and Monet Carlo samples to produce high-quality
306 data, which leads to fast inference. For validation, CWLF is assessed on two public datasets and
307 achieves competitive results compared with existing methods.

308 One limitation of CLWF is that the samples obtained are not diverse enough as we use ODE for
309 inference, which results in slightly higher test (continuous ranked probability score) CRPS compared
310 to previous works, e.g., CSDI. Therefore, for future work, we will seek suitable approaches to
311 accurately model the diffusion term in the SDE. Moreover, we will also try to design better task-
312 specific potential functions for sparse multivariate time series data. We plan to explore the potential
313 of the Lagrangian Wasserstein Flow model for other time series analysis tasks, such as anomaly
314 detection and uncertainty quantification.

315 In terms of broader impact, our study on time series imputation has the potential to address important
316 real-world challenges and consequently make a positive impact on daily lives.

317 **References**

- 318 [1] Michael S Albergo, Nicholas M Boffi, and Eric Vanden-Eijnden. Stochastic interpolants: A
319 unifying framework for flows and diffusions. *arXiv preprint arXiv:2303.08797*, 2023.
- 320 [2] Michael Samuel Albergo and Eric Vanden-Eijnden. Building normalizing flows with stochastic
321 interpolants. In *The Eleventh International Conference on Learning Representations*, 2023.
- 322 [3] Vladimir Igorevich Arnol'd. *Mathematical methods of classical mechanics*, volume 60. Springer
323 Science & Business Media, 2013.
- 324 [4] Richard Bellman. Dynamic programming. *science*, 153(3731):34–37, 1966.
- 325 [5] Julius Berner, Lorenz Richter, and Karen Ullrich. An optimal control perspective on diffusion-
326 based generative modeling. *Transactions on Machine Learning Research*, 2024.
- 327 [6] Dimitri Bertsekas. *Dynamic programming and optimal control: Volume I*, volume 4. Athena
328 scientific, 2012.
- 329 [7] Marin Biloš, Kashif Rasul, Anderson Schneider, Yuriy Nevmyvaka, and Stephan Günnemann.
330 Modeling temporal data as continuous functions with stochastic process diffusion. In *International
331 Conference on Machine Learning*, pages 2452–2470. PMLR, 2023.
- 332 [8] George Casella and Christian P Robert. Rao-blackwellisation of sampling schemes. *Biometrika*,
333 83(1):81–94, 1996.
- 334 [9] Ricky TQ Chen, Yulia Rubanova, Jesse Bettencourt, and David K Duvenaud. Neural ordinary
335 differential equations. *Advances in neural information processing systems*, 31, 2018.
- 336 [10] Tianrong Chen, Guan-Horng Liu, and Evangelos Theodorou. Likelihood training of schrödinger
337 bridge using forward-backward sdes theory. In *International Conference on Learning Representations, 2022*, 2022.
338
- 339 [11] Yongxin Chen, Tryphon T Georgiou, and Michele Pavon. Stochastic control liaisons: Richard
340 sinkhorn meets gaspard monge on a schrodinger bridge. *Siam Review*, 63(2):249–313, 2021.
- 341 [12] Yu Chen, Wei Deng, Shikai Fang, Fengpei Li, Nicole Tianjiao Yang, Yikai Zhang, Kashif Rasul,
342 Shandian Zhe, Anderson Schneider, and Yuriy Nevmyvaka. Provably convergent schrödinger
343 bridge with applications to probabilistic time series imputation. In *International Conference on
344 Machine Learning*, pages 4485–4513. PMLR, 2023.
- 345 [13] Marco Cuturi. Sinkhorn distances: Lightspeed computation of optimal transport. *Advances in
346 neural information processing systems*, 26, 2013.
- 347 [14] Valentin De Bortoli, James Thornton, Jeremy Heng, and Arnaud Doucet. Diffusion schrödinger
348 bridge with applications to score-based generative modeling. *Advances in Neural Information
349 Processing Systems*, 34:17695–17709, 2021.
- 350 [15] Lawrence C Evans. *Partial differential equations*, volume 19. American Mathematical Society,
351 2022.
- 352 [16] Lawrence C Evans. An introduction to mathematical optimal control theory spring, 2024
353 version. *Lecture notes available at <https://math.berkeley.edu/evans/control.course.pdf>*, 2024.
- 354 [17] Wendell H Fleming and Raymond W Rishel. *Deterministic and stochastic optimal control*,
355 volume 1. Springer Science & Business Media, 2012.
- 356 [18] Vincent Fortuin, Dmitry Baranchuk, Gunnar Rätsch, and Stephan Mandt. Gp-vae: Deep
357 probabilistic time series imputation. In *International conference on artificial intelligence and
358 statistics*, pages 1651–1661. PMLR, 2020.
- 359 [19] Nikita Gushchin, Alexander Kolesov, Alexander Korotin, Dmitry P Vetrov, and Evgeny Burnaev.
360 Entropic neural optimal transport via diffusion processes. *Advances in Neural Information
361 Processing Systems*, 36, 2024.

- 362 [20] Jonathan Ho, Ajay Jain, and Pieter Abbeel. Denoising diffusion probabilistic models. *Advances*
363 *in neural information processing systems*, 33:6840–6851, 2020.
- 364 [21] Lars Holdijk, Yuanqi Du, Ferry Hooft, Priyank Jaini, Berend Ensing, and Max Welling. Stochas-
365 tic optimal control for collective variable free sampling of molecular transition paths. *Advances*
366 *in Neural Information Processing Systems*, 36, 2023.
- 367 [22] Diederik P. Kingma and Max Welling. Auto-encoding variational bayes. In *The Second*
368 *International Conference on Learning Representations*, 2014.
- 369 [23] Marcel Kollovich, Abdul Fatir Ansari, Michael Bohlke-Schneider, Jasper Zschiegner, Hao
370 Wang, and Yuyang Bernie Wang. Predict, refine, synthesize: Self-guiding diffusion models for
371 probabilistic time series forecasting. *Advances in Neural Information Processing Systems*, 36,
372 2024.
- 373 [24] Takeshi Koshizuka and Issei Sato. Neural lagrangian schrödinger bridge: Diffusion modeling for
374 population dynamics. In *The Eleventh International Conference on Learning Representations*,
375 2022.
- 376 [25] Christian Léonard. From the schrödinger problem to the monge–kantorovich problem. *Journal*
377 *of Functional Analysis*, 262(4):1879–1920, 2012.
- 378 [26] Lequan Lin, Zhengkun Li, Ruikun Li, Xuliang Li, and Junbin Gao. Diffusion models for time-
379 series applications: a survey. *Frontiers of Information Technology & Electronic Engineering*,
380 pages 1–23, 2023.
- 381 [27] Yaron Lipman, Ricky TQ Chen, Heli Ben-Hamu, Maximilian Nickel, and Matthew Le. Flow
382 matching for generative modeling. In *The Eleventh International Conference on Learning*
383 *Representations*, 2022.
- 384 [28] Guan-Horng Liu, Yaron Lipman, Maximilian Nickel, Brian Karrer, Evangelos Theodorou,
385 and Ricky TQ Chen. Generalized schrödinger bridge matching. In *The Twelfth International*
386 *Conference on Learning Representations*, 2024.
- 387 [29] Qiang Liu. Rectified flow: A marginal preserving approach to optimal transport. *arXiv preprint*
388 *arXiv:2209.14577*, 2022.
- 389 [30] Xingchao Liu, Chengyue Gong, and Qiang Liu. Flow straight and fast: Learning to generate
390 and transfer data with rectified flow. In *The Eleventh International Conference on Learning*
391 *Representations*, 2022.
- 392 [31] Xingchao Liu, Lemeng Wu, Mao Ye, and Qiang Liu. Learning diffusion bridges on constrained
393 domains. In *international conference on learning representations (ICLR)*, 2023.
- 394 [32] Caspar Meijer and Lydia Y Chen. The rise of diffusion models in time-series forecasting. *arXiv*
395 *preprint arXiv:2401.03006*, 2024.
- 396 [33] Kirill Neklyudov, Rob Brekelmans, Daniel Severo, and Alireza Makhzani. Action matching:
397 Learning stochastic dynamics from samples. In *International Conference on Machine Learning*,
398 pages 25858–25889. PMLR, 2023.
- 399 [34] Kirill Neklyudov, Rob Brekelmans, Alexander Tong, Lazar Atanackovic, Qiang Liu, and Alireza
400 Makhzani. A computational framework for solving wasserstein lagrangian flows. *arXiv preprint*
401 *arXiv:2310.10649*, 2023.
- 402 [35] Nikolas Nüsken and Lorenz Richter. Solving high-dimensional hamilton–jacobi–bellman pdes
403 using neural networks: perspectives from the theory of controlled diffusions and measures on
404 path space. *Partial differential equations and applications*, 2(4):48, 2021.
- 405 [36] Bernt Oksendal. *Stochastic differential equations: an introduction with applications*. Springer
406 Science & Business Media, 2013.
- 407 [37] Derek Onken, Samy Wu Fung, Xingjian Li, and Lars Ruthotto. Ot-flow: Fast and accurate
408 continuous normalizing flows via optimal transport. *Proceedings of the AAAI Conference on*
409 *Artificial Intelligence*, 35(10):9223–9232, 2021.

- 410 [38] Gabriel Peyré, Marco Cuturi, et al. Computational optimal transport: With applications to data
411 science. *Foundations and Trends® in Machine Learning*, 11(5-6):355–607, 2019.
- 412 [39] Aram-Alexandre Pooladian, Heli Ben-Hamu, Carles Domingo-Enrich, Brandon Amos, Yaron
413 Lipman, and Ricky TQ Chen. Multisample flow matching: Straightening flows with minibatch
414 couplings. In *International Conference on Machine Learning*, pages 28100–28127. PMLR,
415 2023.
- 416 [40] Hannes Risken and Till Frank. *The Fokker-Planck Equation: Methods of Solution and Applica-*
417 *tions*, volume 18. Springer Science & Business Media, 2012.
- 418 [41] Filippo Santambrogio. Optimal transport for applied mathematicians. *Birkäuser, NY*, 55(58-
419 63):94, 2015.
- 420 [42] Ikaro Silva, George Moody, Daniel J Scott, Leo A Celi, and Roger G Mark. Predicting in-
421 hospital mortality of icu patients: The physionet/computing in cardiology challenge 2012. In
422 *2012 Computing in Cardiology*, pages 245–248. IEEE, 2012.
- 423 [43] Yang Song, Jascha Sohl-Dickstein, Diederik P Kingma, Abhishek Kumar, Stefano Ermon, and
424 Ben Poole. Score-based generative modeling through stochastic differential equations. In
425 *International Conference on Learning Representations*, 2020.
- 426 [44] Yusuke Tashiro, Jiaming Song, Yang Song, and Stefano Ermon. Csd: Conditional score-based
427 diffusion models for probabilistic time series imputation. *Advances in Neural Information*
428 *Processing Systems*, 34:24804–24816, 2021.
- 429 [45] Alexander Tong, Kilian FATRAS, Nikolay Malkin, Guillaume Huguét, Yanlei Zhang, Jarrid
430 Rector-Brooks, Guy Wolf, and Yoshua Bengio. Improving and generalizing flow-based genera-
431 tive models with minibatch optimal transport. *Transactions on Machine Learning Research*,
432 2024. Expert Certification.
- 433 [46] Alexander Tong, Nikolay Malkin, Kilian Fatras, Lazar Atanackovic, Yanlei Zhang, Guillaume
434 Huguét, Guy Wolf, and Yoshua Bengio. Simulation-free schrödinger bridges via score and flow
435 matching. *arXiv preprint arXiv:2307.03672*, 2023.
- 436 [47] Cédric Villani et al. *Optimal transport: old and new*, volume 338. Springer, 2009.
- 437 [48] Liu Yang and George Em Karniadakis. Potential flow generator with l 2 optimal transport
438 regularity for generative models. *IEEE Transactions on Neural Networks and Learning Systems*,
439 33(2):528–538, 2020.
- 440 [49] Jiongmin Yong and Xun Yu Zhou. *Stochastic controls: Hamiltonian systems and HJB equations*,
441 volume 43. Springer Science & Business Media, 2012.
- 442 [50] Qinsheng Zhang and Yongxin Chen. Path integral sampler: A stochastic control approach for
443 sampling. In *The Tenth International Conference on Learning Representations*. OpenReview.net,
444 2022.
- 445 [51] Yu Zheng, Furui Liu, and Hsun-Ping Hsieh. U-air: When urban air quality inference meets
446 big data. In *Proceedings of the 19th ACM SIGKDD international conference on Knowledge*
447 *discovery and data mining*, pages 1436–1444, 2013.

448 A Stochastic Optimal Control

449 The data generation task can also be interpreted as a stochastic optimal control (SOC) problem
450 [4, 17, 35, 50, 21, 5] whose cost function \mathcal{J} is defined as:

$$\mathcal{J}(X_t, t) = \mathbb{E}_{p(X_t)} \left[\int_0^T \int_{\mathbb{R}^d} \frac{1}{2} \|\nabla_x \Psi(X_t, t)\|^2 dX_t dt \right] + \mathbb{E}_{p(X_T)} [\Psi(X_T)], \quad (18)$$

451 where $\frac{1}{2} \|\nabla_x \Psi(X_t, t)\|^2$ denotes the running cost, and $\Psi(X_T)$ denotes the terminal cost. The above
452 SOC problem can be solved by dynamic programming [4, 6].

453 Further, let $V(X_t, t) = \inf \mathcal{J}(X_t, t)$ be the value function/optimal-cost-to-go of the SOC problem,
454 then the corresponding Hamilton-Jacobi-Bellman (HJB) partial differential equation (PDE) [15, 49]
455 is given by

$$\frac{\partial V_t}{\partial t} - \frac{1}{2} \nabla V_t' \nabla V_t + \frac{1}{2} \Delta V_t = 0, \quad (19)$$

$$\text{with the terminal condition: } V(X_t, T) = \Psi(X_t). \quad (20)$$

456 B Rao-Blackwell Theorem

457 **Theorem 1 (Rao-Blackwell)** Let \mathcal{S} be an unbiased estimator of some parameter $\theta \in \Theta$, and $\mathcal{T}(X)$
458 the sufficient statistic for θ , then: 1) $\mathcal{S}^* = \mathbb{E}[\mathcal{S} | \mathcal{T}(X)]$, is an unbiased estimator for θ , and 2)
459 $\mathbb{V}_\theta[\mathcal{S}^*] \leq \mathbb{V}_\theta[\mathcal{S}]$ for all θ . The inequality is strict unless \mathcal{S} is a function of \mathcal{T} .

460 C Experimental Environment

461 For the hardware environment of the experiments, we use a single NVIDIA A100-PCIE-40GB GPU
462 and an Intel(R) Xeon(R) Gold-6248R-3.00GHz CPU. For the software environment, the Python
463 version is 3.9.7, the CUDA version 11.7, and the Pytorch version is 2.0.1.

464 **NeurIPS Paper Checklist**

465 **1. Claims**

466 Question: Do the main claims made in the abstract and introduction accurately reflect the
467 paper’s contributions and scope?

468 Answer: [Yes]

469 **2. Limitations**

470 Question: Does the paper discuss the limitations of the work performed by the authors?

471 Answer: [Yes]

472 Justification: See Sec. 6

473 **3. Theory Assumptions and Proofs**

474 Question: For each theoretical result, does the paper provide the full set of assumptions and
475 a complete (and correct) proof?

476 Answer: [NA]

477 **4. Experimental Result Reproducibility**

478 Question: Does the paper fully disclose all the information needed to reproduce the main ex-
479 perimental results of the paper to the extent that it affects the main claims and/or conclusions
480 of the paper (regardless of whether the code and data are provided or not)?

481 Answer: [Yes]

482 Justification: See supplemental material

483 **5. Open access to data and code**

484 Question: Does the paper provide open access to the data and code, with sufficient instruc-
485 tions to faithfully reproduce the main experimental results, as described in supplemental
486 material?

487 Answer: [Yes]

488 Justification: See supplemental material

489 **6. Experimental Setting/Details**

490 Question: Does the paper specify all the training and test details (e.g., data splits, hyper-
491 parameters, how they were chosen, type of optimizer, etc.) necessary to understand the
492 results?

493 Answer: [Yes]

494 Justification: See supplementary.

495 **7. Experiment Statistical Significance**

496 Question: Does the paper report error bars suitably and correctly defined or other appropriate
497 information about the statistical significance of the experiments?

498 Answer: [Yes]

499 Justification: See Sec. 4

500 **8. Experiments Compute Resources**

501 Question: For each experiment, does the paper provide sufficient information on the com-
502 puter resources (type of compute workers, memory, time of execution) needed to reproduce
503 the experiments?

504 Answer: [Yes] .

505 Justification: See Appendix. C

506 **9. Code Of Ethics**

507 Question: Does the research conducted in the paper conform, in every respect, with the
508 NeurIPS Code of Ethics <https://neurips.cc/public/EthicsGuidelines?>

509 Answer: [Yes]

510 **10. Broader Impacts**

511 Question: Does the paper discuss both potential positive societal impacts and negative
512 societal impacts of the work performed?

513 Answer: [Yes]

514 Justification: See Sec. 6

515 **11. Safeguards**

516 Question: Does the paper describe safeguards that have been put in place for responsible
517 release of data or models that have a high risk for misuse (e.g., pretrained language models,
518 image generators, or scraped datasets)?

519 Answer: [NA] .

520 **12. Licenses for existing assets**

521 Question: Are the creators or original owners of assets (e.g., code, data, models), used in
522 the paper, properly credited and are the license and terms of use explicitly mentioned and
523 properly respected?

524 Answer: [Yes]

525 Justification: See Sec. 4

526 **13. New Assets**

527 Question: Are new assets introduced in the paper well documented and is the documentation
528 provided alongside the assets?

529 Answer: [Yes]

530 **14. Crowdsourcing and Research with Human Subjects**

531 Question: For crowdsourcing experiments and research with human subjects, does the paper
532 include the full text of instructions given to participants and screenshots, if applicable, as
533 well as details about compensation (if any)?

534 Answer: [NA]

535 **15. Institutional Review Board (IRB) Approvals or Equivalent for Research with Human
536 Subjects**

537 Question: Does the paper describe potential risks incurred by study participants, whether
538 such risks were disclosed to the subjects, and whether Institutional Review Board (IRB)
539 approvals (or an equivalent approval/review based on the requirements of your country or
540 institution) were obtained?

541 Answer: [NA] .